

NOTES

Limnol. Oceanogr., 44(2), 1999, 425–430
© 1999, by the American Society of Limnology and Oceanography, Inc.

Pore-water convection induced by peeper emplacement in saline sediment

Abstract—“Peepers” (dialysis samplers) rely on exchange across a dialysis membrane between fluid-filled cells and the surrounding sediment in order to sample the pore water at various depths. In the current study, we show that under some realistic circumstances, where there is a large density difference between the pore water and the cell fluid in permeable sediments, the resulting convective motion in the pore water distorts concentration distributions near the peeper. Peepers withdrawn prematurely in these conditions will contain seriously misrepresentative samples. We present numerical model and laboratory experiment results that show that the equilibration dynamics are complex and that the time required for equilibration may be far in excess of the duration predicted by a simple molecular diffusion model.

A “peeper” (dialysis sampler) consists of a series of cells assembled in a vertical array that is covered with dialysis membrane (Hesslein, 1976) (Fig. 1). The peeper is embedded into aquatic sediment to sample the pore water in order to allow us to construct a concentration profile. Ions in the pore water diffuse across the membrane into the peeper cells, and the peeper is removed when the cell solution reaches equilibrium with the surrounding solution. A major consideration for peeper use is that deployment lasts long enough to ensure that the concentrations within peeper cells accurately reflect those in the undisturbed sediment.

The principal factors influencing the time required to reach equilibrium are the permeation speed of the peeper membrane, the rate of mixing within the peeper cell, and the rate of transport from the surrounding sediment to the membrane surface. Experiments by Webster et al. (1998) demonstrated that a numerical model simulating diffusion through the surrounding sediment was well able to describe the equilibration dynamics of isolated vial peepers. Harper et al. (1997) also modeled peeper equilibration dynamics for three different cases: well buffered (desorption or dissolution from the solid phase to the pore water); diffusion (no resupply from the solid phase); and partial resupply from the solid phase.

Using a numerical model to solve the two-dimensional diffusion equation, we simulated the equilibration behavior of a peeper embedded in sediment with a uniform pore-water concentration. This is equivalent to the second case described above (no resupply), which was considered by Harper et al. (1997). The model predictions were compared to measurements made in mesocosm sediments, from which peepers were withdrawn at daily intervals. The measured peeper concentrations increased at a rate that was several times faster than predicted by the model. Concentrations increased more rapidly in the lowest cells, but our diffusion model predicted faster equilibration in only the lowest cell.

Analogous laboratory experiments showed the same enhanced equilibration. Clearly, the diffusion model is deficient under these circumstances.

A possible explanation is that haline convection in the sediment pore water along the face of the peeper enhances solute transport through the sediment pores. As ions diffuse from the sediment into peeper chambers initially filled with distilled water, the pore water becomes depleted of ions and therefore reduces in density. The lighter pore water floats upward along the face of the peeper, toward the sediment surface, and draws in denser water from further afield. For uniform pore-water concentrations, this shortens the time to equilibrium and brings the lowest cells into equilibrium first. Adler (1977) also observed faster equilibration in the lowest peeper cells, and he too suggested pore-water convection as a possible mechanism. He concluded that peeper water and pore waters should be the same density in order to prevent convection from distorting the results. As yet, this is not normal practice (e.g., Adams 1994). The suggestion has been made that peepers should be filled with a sodium chloride (NaCl) solution that is half the concentration of the NaCl expected at the sampling location, with the intention that a dilute salt solution would reduce osmotic loss from a peeper deployed in a saline environment while still providing a favorable concentration gradient for transporting dissolved species into the peeper (Simon et al. 1985). Clearly this practice would be inappropriate if the sediment is permeable enough to allow pore-water convection.

We conducted laboratory experiments using peepers containing 36 dual-windowed cells, each 10-mm deep, 6-mm high, and 60-mm wide, with a center-to-center separation of 10 mm (Fig. 1). The cells were covered with a 0.45- μm polysulfone membrane. This design is similar to that developed by Hesslein (1976), a design that has been used in geochemical and ecotoxicological studies (Gaillard et al. 1986; Tessier et al. 1989; Williamson and Parnell, 1994; Hare et al. 1994). Six peepers were filled with deionized water and placed in a bin of fine sand containing well-mixed artificial seawater made from NaCl, magnesium chloride, calcium chloride, potassium chloride, sodium bicarbonate, and strontium chloride. The peepers were inserted into the sediment and were removed one at a time over the next 10 d, and the cell contents were analyzed using inductively coupled plasma mass spectroscopy (ICP-MS). We will discuss only the measurements of the magnesium concentration, although our findings are applicable to all species. Magnesium comprised 4% of the original dry mass of species dissolved and is treated as a tracer in our experiments. The porosity and permeability of the sediment were measured to be 0.42 and $3.0 \times 10^{-11} \text{ m}^2$, respectively.

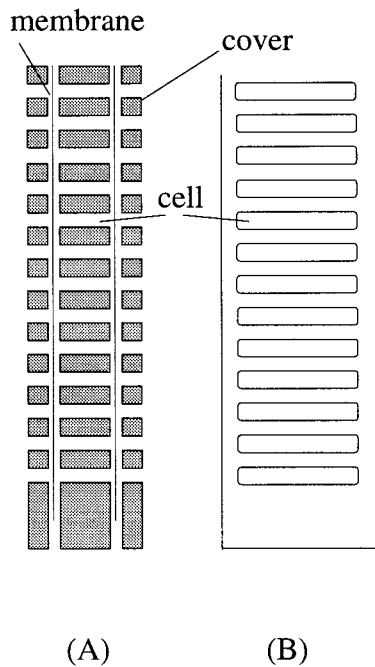


Fig. 1. Diagram of a multi-chambered peeper (not drawn to scale): (A) side view, (B) plan view of the peeper cover.

We constructed a numerical peeper equilibration model to simulate the above experiment. The numerical model simulated an eight-cell dual-window peeper embedded in sandy sediment saturated by a uniform NaCl solution containing a Mg^{2+} tracer. The NaCl concentration in the simulation was set to match the density of artificial seawater used in our experiments. The peeper cells had the same physical dimensions and separation distance as the peeper described above. The model was two-dimensional; any variations across the width of the peeper chamber were ignored. Symmetry allowed us to model this system with 5-mm deep, single-window chambers, considering only the sediment on one side of the peeper (Fig. 2). The model domain extended vertically from the sediment surface to the base of the peeper.

The transport of NaCl and Mg^{2+} was modeled using the advection–diffusion equation

$$\frac{\partial c}{\partial t} + \frac{1}{\varphi} \nabla(\mathbf{u}c) = D_s \nabla^2 c \quad (1)$$

where c is the pore-water concentration, \mathbf{u} is the bulk transport velocity (a vector), φ is the porosity, and D_s is the diffusivity of the solute in the sediment. This diffusivity is lower than the value in free water and is estimated by dividing the free-water value by the tortuosity squared (θ^2). The tortuosity was estimated from the porosity using (Boudreau 1996):

$$\theta^2 \approx 1 - 2 \ln(\varphi) \quad (2)$$

which gives a value of $\theta^2 = 2.7$ for a porosity of 0.42.

We used a forward-time centered-space differencing scheme for the diffusion terms and upwind differencing for the advection terms in Eq. 1 (Roache 1982). The velocities were determined from Darcy's law:

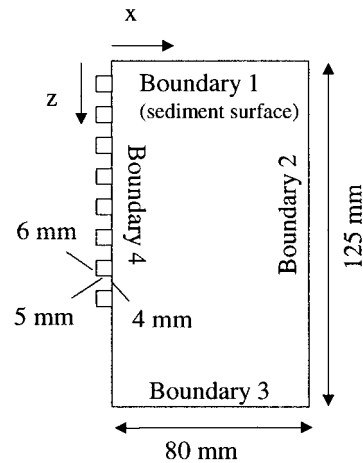


Fig. 2. The model domain for the diffusion and convection models (not to scale).

$$\mathbf{u} = -\frac{k}{\mu} (\nabla p - \rho \mathbf{g}) \quad (3)$$

where p is the pore-water pressure, k is the permeability, μ is the viscosity, and ρ is the pore-water density. The density was assumed to be a linear function of the NaCl concentration.

Combining Eq. 3 with the continuity equation

$$\nabla \cdot \mathbf{u} = 0 \quad (4)$$

gives

$$\nabla^2 p = g \frac{\partial \rho}{\partial z} \quad (5)$$

The model solved this equation for p at each time step using a successive over-relaxation algorithm (Press et al. 1992).

The lower boundary and the vertical boundary furthest from the peeper were assumed to be far enough away that their effects were not “seen” by the peeper face, so a constant concentration condition was applied to these boundaries (boundaries 2 and 3 in Fig. 2). A constant concentration boundary condition was assumed for the sediment–water interface (boundary 1), as the concentration in the overlying water would not vary significantly with time. The solute flux was set to be zero across the solid surface of the peeper (boundary 4). At the chamber windows along boundary 4, a membrane-flux condition was applied,

$$\frac{\partial c_p}{\partial t} = \frac{r}{f} (\bar{c} - c_p) \quad (6)$$

where r is the membrane permeation speed, f is the ratio of the volume of the peeper cell to the membrane area (design factor), c_p is the solute concentration in the peeper cell (assumed to be homogeneous), and \bar{c} is the average pore-water concentration along the surface of the membrane. This condition is derived from the assumption that the flux across the membrane is proportional to the permeation speed multiplied by the concentration difference across the membrane.

The initial pressure distribution was assumed to be hydrostatic, with the surface pressure arbitrarily set and maintained at zero (boundary 1). Again, we assumed that boundaries 2 and 3 were far enough away that they were not seen

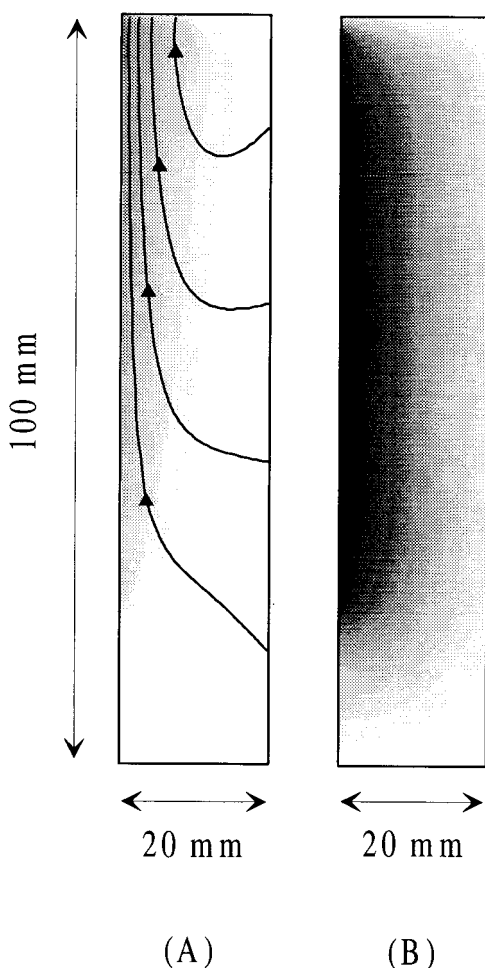


Fig. 3. (A) The NaCl concentration distribution and streamlines close to the peeper cells for the convection model 24 h after peeper deployment. The concentration range is from 25.9 gL^{-1} at the peeper face to 32 gL^{-1} at the far boundaries; (B) The NaCl concentration distribution close to the peeper cells for the diffusion model 24 h after peeper deployment. The concentration ranges from 17.5 gL^{-1} at the peeper face to 32 gL^{-1} at the far boundaries. Concentration is represented by a linear shading scale; white is 0 mg L^{-1} and the darkest shade is 17.5 mg L^{-1} .

by the peeper, so the pressure along these boundaries was also assumed to remain constant in time. There could be no horizontal velocity across the peeper surface, so a condition of zero horizontal pressure gradient was applied on boundary 4.

The stream function ψ , which is a convenient way to represent the interstitial flows, is related to the horizontal and vertical velocities by

$$u = \frac{\partial \psi}{\partial z}; \quad w = -\frac{\partial \psi}{\partial x}. \quad (7)$$

We calculated the stream function for the domain by integrating the vertical velocities out from the peeper surface, assuming a value of zero for the stream function at the peeper surface. The contours of the stream function are the streamlines, which show the direction of the flow. The distance between the streamlines is inversely proportional to the local flow speed; closely spaced streamlines indicate high flow speeds.

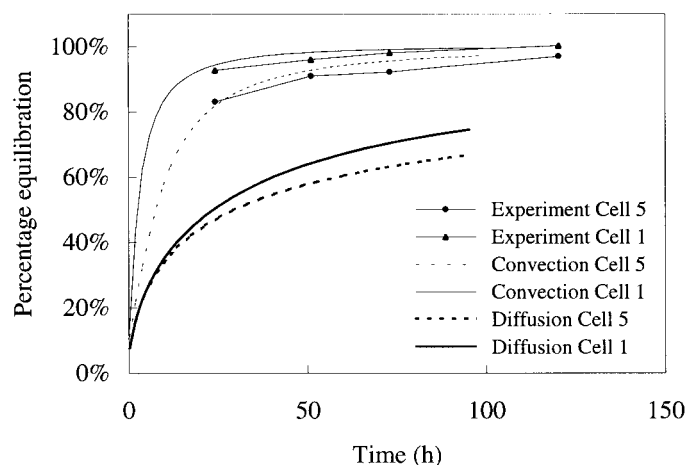


Fig. 4. Time evolution of peeper cell Mg^{2+} concentrations for the convection model, diffusion model, and experiment.

The diffusion model used for comparison is identical to the convection model, except that the velocity is set to zero throughout the model domain. Transport of solute occurs by molecular diffusion only.

We ran the model with an initial condition of uniform NaCl and Mg^{2+} pore-water concentration throughout the sediment and with zero concentration within the peeper cells. The membrane permeation speed was measured by Webster et al. (1998) to be $2.7 \times 10^{-6} \text{ ms}^{-1}$ for bromide ions (diffusing as major ions into fresh water at 23°C). Using data from Li and Gregory (1974), the membrane permeation speeds (r), adjusted for the temperature of our experiment, are estimated to be $2.5 \times 10^{-6} \text{ ms}^{-1}$ and $1.5 \times 10^{-6} \text{ ms}^{-1}$ for NaCl and Mg^{2+} , respectively. We used the measured values for porosity ($\phi = 0.42$) and permeability ($k = 3.0 \times 10^{-11} \text{ m}^2$) in the model.

The convection model predicts an upward flow along the face of the peeper, as illustrated by the streamlines (Fig. 3A). Comparison between NaCl concentration distributions produced by the diffusion and convection models indicates this flow to be sufficient to produce first-order effects on the concentration distribution in the sediment pore water. The drawdown volume, or zone of ionic depletion, differs considerably between the two cases (Fig. 3B). The convection model predicts a drawdown volume that increases in extent from the bottom end of the peeper to the top. Conversely, with the exception of the two zones at the top and bottom of the peeper, the diffusion model predicts that the concentration drawdown in the sediment because of solute diffusion into the peeper cell is approximately uniform along the length of the peeper and is substantially greater than the drawdown when convection is occurring. Convection is effective at replacing pore water depleted in solute near the peeper surface.

The concentrations measured in the peeper experiments are displayed with the predictions from the convection and diffusion models in Fig. 4. We show results for the bottom cell in the peeper (cell 1) and the fifth cell up from the bottom (cell 5). The Mg^{2+} concentration in the experimental peepers approached equilibrium much more rapidly than pre-

dicted by the diffusion model, reaching greater than 80% equilibration after 1 d. The reason for the difference in equilibration times between the diffusion and convection cases is simply that convection is able to maintain elevated solute concentrations along the face of the peeper despite drawdown into the peeper cells, whereas diffusion is a much less effective transport mechanism in this case. The diffusion model predicted less than 50% equilibration by this time. By contrast, the convection model predicts 94 and 82% equilibration after 24 h for cells 1 and 5 compared to measured values of 93 and 83%. It should be noted that the model represents a significant simplification of the experimental setup. For example, the model considers only two dimensions, and it fails to account for the more complex geometry of the slotted guard sheet covering the peeper. Other assumptions, such as uniform porosity and permeability and the limitations of the tortuosity estimate, further limit the model. Despite these assumptions, the model does a credible job of predicting the equilibration behavior of these peepers and is better able to describe our experimental findings than is the diffusion model.

The correspondence between the modeled and observed results suggests that our interpretation of the main transport processes is correct. A simple experiment, first performed in 1993 in collaboration with H. L. Golterman (Arles, France), provides a further test of our hypothesis. Agar strips dyed with fluorescein were placed in four peeper cells of a 36-celled peeper. All the cells were filled with distilled water, covered with dialysis membrane, and the peeper was inserted into sediment saturated with artificial seawater. The sediment-water interface was located at the midpoint of cell 21 (where cell 1 is at the base of the peeper). The agar strips were inserted into cells 5, 10, 15, and 20. The peeper was removed after 24 h, the cell solutions were sampled, and the concentration of fluorescein was determined from absorption spectrophotometry. Our measurements demonstrated that over the 24-h period, fluorescein had been transported to neighboring peeper cells (Fig. 5). We also observed that the fluorescein transport was not vertically symmetrical, and cells immediately above an agar-filled cell contained higher fluorescein concentrations than those immediately below the cell.

We suggest that fluorescein diffused out of the cells containing the dye into the nearby pore water, was transported upward by convection along the face of the peeper, and then diffused back across the dialysis membranes of neighboring cells. That the cells above the cells initially containing the fluorescein contained more dye than those below is consistent with this hypothesis. Transport governed by diffusion only would result in a vertically symmetric exchange between a cell and its two neighbors.

Webster et al (1998) found advantages in filling large dialysis chambers with distilled water for deployment in marine sediments, as the haline convection induced within the cells greatly reduces the internal mixing time. Our present results suggest that caution is required in permeable sediments, as such density differences may induce significant haline convection in the pore water as well as within the peeper cells.

If the peeper is kept in the sediment for long enough, the density differences reduce, thereby weakening the vertical

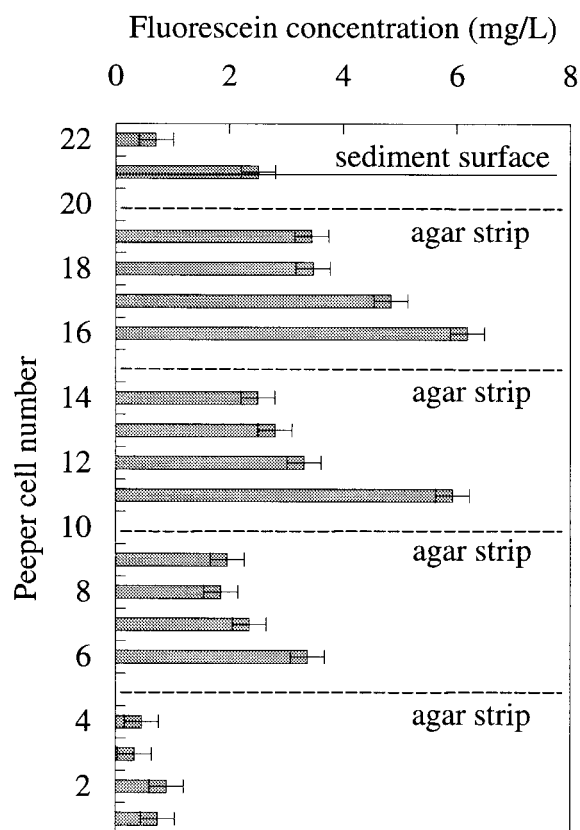


Fig. 5. Fluorescein concentration in each peeper cell 24 h after peeper deployment. The position of the sediment surface and of the cells containing agar strips are indicated.

velocity. Once the velocity is effectively zero, diffusion controls the transport of ions, and the peeper eventually reaches the "correct" equilibrium with the surrounding pore water. Given this scenario, one might suppose that an appropriate deployment duration could be estimated from the diffusion model. Additional model results suggest that even this seemingly conservative estimate may significantly underestimate the time required to acquire representative pore-water samples.

The convection model was applied to investigate the effect of convection on the equilibration of peepers to a Mg^{2+} concentration field, which initially decreased linearly with depth. In the simulations, the concentrations of Mg^{2+} were maintained at their initial values along boundaries 1, 3, and 4 so that in the absence of a peeper, the concentration profile of Mg^{2+} would remain linear and constant for all time. The initial, uniform NaCl concentration field and boundary conditions remained unchanged. The Mg^{2+} concentration fields 100 h after peeper deployment predicted by the diffusion and convection models are illustrated in Fig. 6. On first inspection, the concentration fields appear to be similar for the two models. In both cases, the concentration contours are deflected vertically near the peeper surface. In the diffusion model, this deflection is caused by drawdown in the vicinity of the peeper cells (Fig. 6B). In the convection model, the effect is more pronounced, due to both drawdown and to the vertical advection of lower concentration pore water from below (Fig.

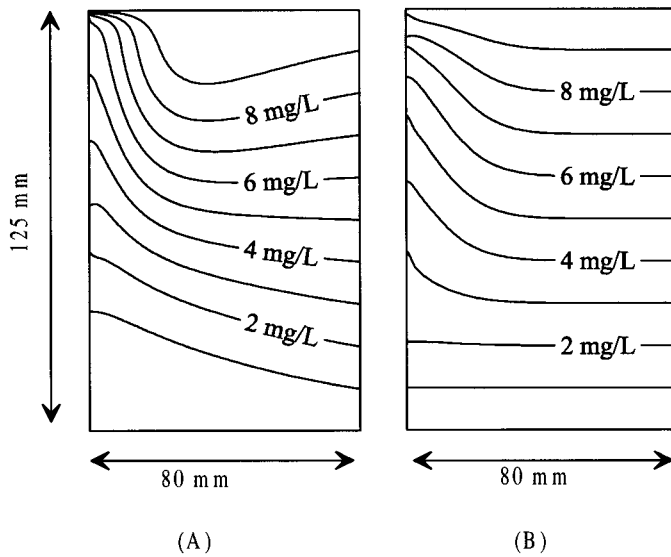


Fig. 6. (A) Effect of convection on linear Mg^{2+} concentration field 100 h after peeper deployment. (B) Effect of diffusion on the same initial concentration field 100 h after peeper deployment. In both graphs, the concentration range is from 0 gL^{-1} along the bottom boundary to 0.01 gL^{-1} along the surface.

6A). For example, the 5 mg/liter contour in Fig. 6A meets the peeper surface at a point 13 mm higher than in Fig. 6B).

Initially, pore water of relatively high concentration was transported across the peeper membranes into the cells. The convection initially served to quicken this process by replenishing the pore water near each cell more rapidly. After some time, the vertical flow along the peeper face transported low concentration fluid up from below the lowest cell. In the scenario we modeled, this concentration was lower than the concentration within some of the cells, and the cell concentrations subsequently decreased or leveled out (Fig. 7). After 200 h, the peeper concentrations were considerably lower than predicted by the diffusion model. Although the peeper will eventually come to equilibrium with the surrounding pore water, the transport dynamics are such that the length of time required may be far in excess of the duration estimated from the diffusion-only model. Convection increases the volume of fluid whose concentrations have been altered by the presence of the peeper compared to the volume affected if diffusion is the sole transport mechanism. Equilibration is not attained until diffusion has reset the concentration profile to something similar to its condition before the peeper was installed.

It would appear that the rapid equilibration behavior demonstrated by the experimental peepers inserted into sediment having uniform solute concentration (Fig. 4) is not equilibration with nearby pore waters at all. Rather, rapid equilibration is achieved by drawing pore water from other depths within the sediment. Nonuniform profiles are certain to have very different equilibration behavior.

Pore-water velocity depends on the sediment permeability (Eq. 3), which is related to sediment properties such as the porosity and the size, shape, and arrangement of particles. For example, typical permeabilities for clean sand range be-

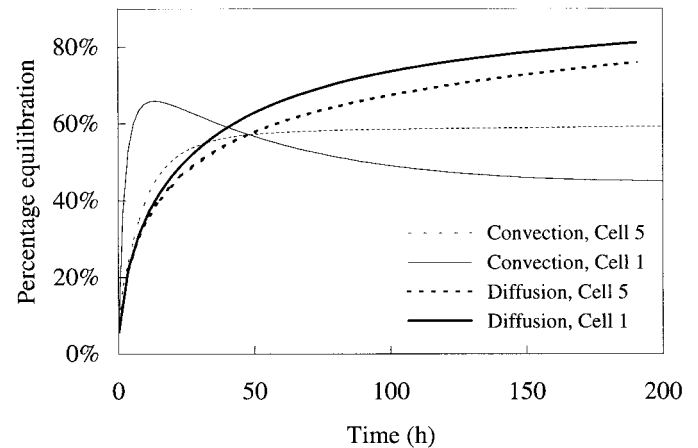


Fig. 7. Time evolution to equilibrium of peepers in a linear concentration field. Comparison with diffusion path to equilibrium. The percentage equilibration is the ratio of the Mg^{2+} concentration to the initial pore-water value at that depth.

tween 10^{-9} – 10^{-12} m^2 , and the range for silt is 10^{-12} – 10^{-16} m^2 (Bear 1972). In our experiments, conducted in fine sand, we have seen that the permeability is high enough that convection velocities are significant. We also ran the model using measured permeability and porosity values ($k = 5.4 \times 10^{-12} \text{ m}^2$ and $\phi = 0.38$) from North Sea sediment, described as muddy sand (Ziebis et al. 1996). We found that the effects of convection were still important, despite the lower permeability. For example, at $t = 200 \text{ h}$, the cell NaCl concentrations (cells 1 to 5) were between 15 and 20% higher than the equivalent diffusion model concentrations. This emphasizes the need for caution where substantial density differences exist between the peeper cells and pore water. Under appropriate conditions (fine mud, for example), peepers may be used effectively without fear of convection distorting results. The following scaling analysis provides an approximate guide to assess the risk of convective transport.

The zone of solute drawdown in the sediment in the vicinity of a single peeper cell near equilibration will be approximately a half cylinder of sediment whose axis lies horizontally along the peeper window. We estimate a length scale for solute drawdown as the radius, R , of the half cylinder that has the same interstitial volume as the peeper cell. If the cell depth is l and its height is h , then the length scale is calculated as

$$R = \sqrt{\frac{2hl}{\pi\phi}} \quad (8)$$

The time scale for transport by diffusion across this distance is

$$T_d \sim \frac{R^2}{\phi D_s} \quad (9)$$

Based on Darcy's law, given by Eq. 3, a vertical velocity scale for the pore water along the peeper surface is

$$w_p \sim \frac{kg'}{v} \quad (10)$$

where k is the sediment permeability, ν is the kinematic viscosity, and $g' = g\Delta\rho/\rho$ is reduced gravity where $\Delta\rho$ is the density difference between the cell fluid and pore water and ρ is the density of the cell fluid.

The time taken for pore water to travel at this velocity across R is then

$$T_c \sim \frac{\nu R}{kg'} \quad (11)$$

A Péclet number, Pe (the ratio of diffusive to convective time scales), can be defined as

$$Pe = \frac{T_d}{T_c} = \frac{Rkg'}{\nu\phi D_s} \quad (12)$$

The Péclet number was approximately 350 for the scenario we modeled. We ran the model using a reduced permeability of 10^{-13} m^2 (which corresponds to $Pe = 1.2$) and found that the differences between this case and the diffusion-only scenario were negligible. Increasing the Péclet number to 10 produced markedly different results. For example, after 100 h, the concentrations in the cells were between 20 and 5% lower than at this time in the diffusion-only run.

In deriving our length scale for solute drawdown, we have assumed that there is no resupply or desorption from the sediment grains. If there is desorption from the sediment, the drawdown radius will be smaller than the above estimate, and so the Péclet number will be reduced. For this reason, the no-resupply case we have presented should be viewed as a worst-case scenario.

Our model simulations and laboratory experiments demonstrate that peeper deployment in permeable, saline sediment where the cells are filled with pure water may induce significant density-driven pore-water convection next to the peeper. Such convection is well able to create a significant shift in the concentration distributions within the sediment. Under some circumstances, the shifted concentration field requires a considerable length of time to dissipate, and so the time required for the peeper to come to the correct equilibrium may be much greater than the time predicted if diffusion is the only transport mechanism. A peeper removed before this time will contain unrepresentative samples, and the inferred concentration profile will be seriously in error. Deploying a peeper containing a tracer such as fluorescein dye in one of its cells may be useful; an asymmetric distribution of fluorescein in the resulting profile would indicate that pore-water convection has occurred. A practical technique to minimize the effects may be to fill cells with a solution that has the same density as the pore water to be sampled. The density should be matched by ensuring that the concentrations of the major ions contributing to the pore-water density are equal to the pore-water concentrations. This approach will minimize problems but may not eliminate them, particularly in estuarine sediments, where it is difficult to match in situ pore-water density gradients.

Nicola J. Grigg

CSIRO Land and Water
GPO Box 1666
Canberra ACT 2601, Australia;
and the Centre for Resource and Environmental Studies
Australian National University
Canberra ACT 0200, Australia

Ian T. Webster and Phillip W. Ford

CSIRO Land and Water
GPO Box 1666
Canberra ACT 2601, Australia

References

- ADAMS, D. D. 1994. Sediment pore water sampling, p. 171–202. *In* A. Mudroch and S. D. MacKnight [eds.], *Handbook of techniques for aquatic sediments sampling*, 2nd ed. CRC Press.
- ADLER, D. M. 1977. Use of the “peeper” to measure diffusion and reaction rates in pore waters. Masters thesis, Columbia University.
- BEAR, J. 1972. *Dynamics of fluids in porous media*. Elsevier.
- BOUDREAU, B. P. 1996. The diffusive tortuosity of fine-grained un lithified sediments. *Geochim. Cosmochim. Acta* **60**: 3139–3142.
- GAILLARD, J. F., C. JEANDEL, G. MICHARD, E. NICOLAS, AND D. RENARD. 1986. Interstitial water chemistry of Villefranche Bay sediments: Trace metal diagenesis. *Mar. Chem.* **18**: 233–247.
- HARE, L., R. CARIGNAN, AND M. A. HUERTADIAZ. 1994. A field study of metal toxicity and accumulation by benthic invertebrates—implications for the acid volatile sulfide (AVS) model. *Limnol. Oceanogr.* **39**:1653–1668.
- HARPER, M. P., W. DAVISON, AND W. TYCH. 1997. Temporal, spatial, and resolution constraints for *in situ* sampling devices using diffusional equilibration—dialysis and DET. *Environ. Sci. Technol.* **31**: 3110–3119.
- HESSLEIN, R. H. 1976. An *in situ* sampler for close interval pore water studies. *Limnol. Oceanogr.* **21**: 912–914.
- LI, Y., AND S. GREGORY. 1974. Diffusion of ions in sea water and in deep-sea sediments. *Geochim. Cosmochim. Acta* **38**: 703–714.
- PRESS, W. H., S. A. TEUKOLSKY, W. T. VETTERLING, AND B. P. FLANNERY. 1992. *Numerical recipes in FORTRAN: The art of scientific computing*. Cambridge University Press.
- ROACHE, P. J. 1982. *Computational fluid dynamics*. Hermosa.
- SIMON, N. S., M. M. KENNEDY, AND C. S. MASSONI. 1985. Evaluation and use of a diffusion-controlled sampler for determining chemical and dissolved oxygen gradients at the sediment-water interface. *Hydrobiologia* **126**: 135–141.
- TESSIER, A., R. CARIGNAN, B. DUBREUIL, AND F. RAPIN. 1989. Partitioning of zinc between the water column and the oxic sediments in lakes. *Geochim. Cosmochim. Acta* **53**: 1511–1522.
- WEBSTER, I. T., P. R. TEASDALE, AND N. J. GRIGG. 1998. A theoretical and experimental analysis of peeper equilibration dynamics. *Environ. Sci. Technol.* **32**: 1727–1733.
- WILLIAMSON, M. A., R. A. PARNELL, JR. 1994. Partitioning of copper and zinc in the sediments and porewaters of a high-elevation alkaline lake, east-central Arizona USA. *Appl. Geochem.* **9**: 597–608.
- ZIEBIS, W., M. HUETTEL, AND S. FORSTER. 1996. Impact of biogenic sediment topography on oxygen fluxes in permeable seabeds. *Mar. Ecol. Prog. Ser.* **140**: 227–237.

Received: 20 April 1998

Accepted: 23 September 1998

Amended: 19 October 1998

Acknowledgments

We thank Graeme Batley and Simon Apte (CSIRO Division of Coal and Energy Technology) for the ICP-MS analyses and helpful comments on an earlier draft. Our thanks also to Robin Wooding for his review and comments. We are grateful to Bernard Boudreau and two anonymous reviewers for their careful reviews and constructive comments.